Materials Science in Semiconductor Processing 147 (2022) 106738

Contents lists available at ScienceDirect

Materials Science in Semiconductor Processing

journal homepage: www.elsevier.com/locate/mssp

# Supercapacitor behaviors of carbon quantum dots by green synthesis method from tea fermented with kombucha

Canan Baslak [a,*], Serkan Demirel [b,**], Adem Kocyigit [c], Hamdiye Alatli [d], Murat Yildirim [d]

[a] Selçuk University, Science Faculty, Department of Chemistry, Konya, Turkey
[b] Igdir University, Vocational High School, Department of Electric and Energy, Igdir, Turkey
[c] Bilecik Seyh Edebali University, Vocational High School, Department of Electronic and Automation, Bilecik, Turkey
[d] Selçuk University, Science Faculty, Department of Biotechnology, Konya, Turkey

ARTICLE INFO

*Keywords:*
Kombucha fungus
Carbon quantum dots
Supercapacitors
Electrode materials

ABSTRACT

Quantum dots have good optical and electronic behaviors due to their smaller size and having changeable properties depending on the size owing to quantum confinement effect. They can be used in various applications such as solar cells, drug delivery, displays and supercapacitors. In this study, carbon quantum dots (CQD) with nitrogen containing have been synthesized by green synthesize technique from the Kombucha fungus and characterized by HRTEM, XRD, XPS, particle sizer, luminescence and UV–Vis spectrometers. While the XRD results confirmed the crystalline structure of the CQDs, HRTEM results revealed the size of CQDs as 5 nm. The luminescence spectroscopy results showed blue-green emission. The UV–Vis spectrometer affirmed absorption peaks of the carbon at around 250–330 nm wavelengths. The CQDs were used as electrode materials for supercapacitor structure and characterized by electrochemical analysis to determine charge-discharge profiles and capacity. The results revealed that the green synthesized CQDs can be employed and improved for supercapacitor applications.

## 1. Introduction

The Kombucha obtained from infusion of tea leaves by the fermentation is a symbiosis of bacteria and various yeasts [1–4]. Kombucha consists of various tea fungus such as Cainii kvass, Cainiigrib, Kambucha, Jsakvasska, Japonskigrib, Heldenpilz, Kombuchaschwamm and Funkochinese. Tea fermented with kombucha is a carbonated, slightly sweet and acidic beverage consumed worldwide. This fermentation is carried out at room temperature for 7–14 days in sugared tea [4]. Kombucha is a non-toxic fungus that grows easily and quickly, and its popularity has become an effective tool for scientists in recent years [5–7].

Carbon quantum dots (CQDs), a new fluorescent nanomaterial with below 10 nm sizes, have attracted much attention owing to their high photostability, good dispensability in aqueous solutions, easy functionalization, high resistance against to photo-bleaching, low cytotoxicity, suitability for bioimaging and drug delivery, and their unique compatibility in photovoltaic production [8–13]. This new type of fluorescent nanomaterials, contain a carbon core and functional groups coated on their surface [14]. Due to their high fluorescence emission and wide excitation spectra, CQDs are excellent donors for fluorescence resonance energy.

Synthesis of nanomaterials especially quantum dots is divided into two classes as top-down and bottom-up approaches according to the different precursors. Generally, the bottom-up methods refer to the pyrolysis of small molecules under hydrothermal and solvothermal conditions [15–18]. These methods can be used for green synthesize of the CQDs.

Supercapacitors have gained great interest due to their much higher capacitance values than the normal capacitors and their better applications in vehicles, elevators, flashes for cameras and biomedical devices [19,20]. Supercapacitor structures have two electrodes, an electrolyte and separator materials, and these materials have been studied over the years for obtaining better performance [21]. Among them, the electrode materials can be developed by synthesizing more porous surfaces to load more charges on them [22]. The CQDs with porous surfaces can be employed for improving of the supercapacitor performance as electrode materials [23]. In addition, CQDs support a

* Corresponding author.
** Corresponding author.
*E-mail addresses:* cananbaslak@hotmail.com (C. Baslak), serkan.demirel@igdir.edu.tr (S. Demirel).

https://doi.org/10.1016/j.mssp.2022.106738
Received 18 November 2021; Received in revised form 18 April 2022; Accepted 19 April 2022
Available online 25 April 2022
1369-8001/© 2022 Elsevier Ltd. All rights reserved.

higher surface infiltration rate than other materials [24]. This may support the electrode-electrolyte interactions, increasing the capacitive polarization and positively affect the capacitance levels [24–26].

In this study, we synthesized CQDs by green synthesize method from the Kombucha fungus successfully, and used them as electrode materials for supercapacitor structure. The CV measurements were performed on the CQDs supercapacitor for various scan speeds to obtain capacity and charge-discharge profiles for high cycle levels.

## 2. Experimental

### 2.1. Materials

All chemicals used in this study were commercially purchased and used as pure grade without further purification. Kombucha fungus was grown up in our laboratory after purchasing. Ethylene diamine (99%, EDA) and filter papers were purchased from Sigma-Aldrich. Milli-Q water was used in all synthesis and spectroscopic measurements.

### 2.2. Synthesis of fluorescent CQDs

Standard mushroom growing procedure: 1 L of tap water was boiled and approximately 50 g of sugar (sucrose) was mixed into the water during boiling. Sugared water was poured into a glass bottle which was previously sterilized with boiling water. Then, about 5–6 g of tea leaves were added into glass bottle, and after 5 min of infusion, the tea leaves were filtered and removed. Approximately 24 g of tea mushrooms (culture) were added into the tea solution, and the solution was cooled down to room temperature (20 °C). 100 ml of the culture water of the fungus was added into the tea mixture and left for fermentation. The fermented tea with kombucha mushroom was kept in fermentation for approximately 20 days. The glass container was covered with a cloth to trap insects and stored for fermentation [2]. After fermentation, the tea was filtered and separated from the mushroom. 0.2 ml of EDA was added to 50 ml of the fermented tea. The tea-EDA mix solution was stirred vigorously. Low emission under UV-light was observed after 2 h. It was determined that particles were formed with intense green emission under UV-light after stirring about 5 h. The light-yellow aqueous solution of CQDs with nitrogen containing was filtered by a 0.2 mm porous size filter. The solution was stored at 4 °C for further characterization and characterization [4,27,28]. The image of the Kombucha fungi used for the synthesis is shown in Fig. 1. The fungus was waited in a stack and the fermentation continued in the bottle. These fungi have been left for fermentation for more than 15 days. A suitable portion of the fungi was taken, and an aqueous solution was prepared and used for CQDs.

### 2.3. Instruments and characterization

Spectral properties of the CQDs were measured by using a PerkinElmer Lambda 25 UV–vis spectrophotometer and PerkinElmer LS 55 luminescence spectrometer in a standard quartz cuvette, respectively. A JEOL JEM 2100 FHRTEM brand high-resolution tunneling electron microscopy (HRTEM) studies were performed for imaging of carbon nanoparticles. Crystallinity of CQDs was studied using Bruker Advance D8 X-ray diffraction spectroscopy (XRD) instrument with Cu Ka radiation at a scan rate of 2°/min for 2 $\theta$ between 10° and 80°. The elemental composition of CQDs was studied using X-ray Photoelectron Spectroscopy (XPS) equipped with a monochromatic Al/Kα (Thermo-K-Alpha) as the X-ray source. Particle size was measured by using MALVERN/DLS MPT2 brand Dynamic Light Scattering (DLS).

### 2.4. Electrochemical capacitor measurements of fluorescent CQDs

The electrochemical capacitor measurements were conducted with Gamry 1010-E galvanostat/potentiostat. The Swagellok-type cell was used for capacitor analysis. In order to measure electrode properties,

**Fig. 1.** Image of Kombucha fungus in fermentation bottle.

two equal amounts (0.01 g) of CQDs were dropped on the two same 1 cm diameter stainless-steel foils. They were used as current collector electrodes because of having high conductivity and high surface resistance, and prevent the electrodes from redox reactions between sample-current collectors. Therefore, the maximum capacitance values were obtained from CQDs. Furthermore, 6 M KOH aqueous solution and cellulosic paper membrane was used as electrolyte and membrane, respectively. The cyclic voltammetry (CV) measurements were carried out for constant scan speeds of 100, 200, 400 and 800 mV/s. The CV measurements were conducted as 3 cycles to observe any anomalies, but only one CV cycle data was given in the result section to avoid data analyses confusion. In order to measure the capacitance, the two-electrode method was exploited. The cycle life study capacitance measurements were performed under 200 mV/s constant scanning speed in the range of 0–1 V for 200 cycles. Then, capacitance values of the samples are calculated with Eq. (1) in the reference of CV results [29].

$$C = \frac{\int IdV}{2m\Delta V v} \tag{1}$$

where $I$ is current, $m$ is electrode active material weight, $\upsilon$ is scan rate, and $\Delta V$ is voltage range.

## 3. Results and discussion

### 3.1. Characterization of fluorescent CQDs

A series of successive characterizations were performed to gain insight into the fluorescence mechanism and structural properties of the CQDs described here. The absorption peak obtained by the UV–vis spectroscopy method, which allows to easily analyze the optical properties of CQDs, have been seen in Fig. 2. CQDs have showed the

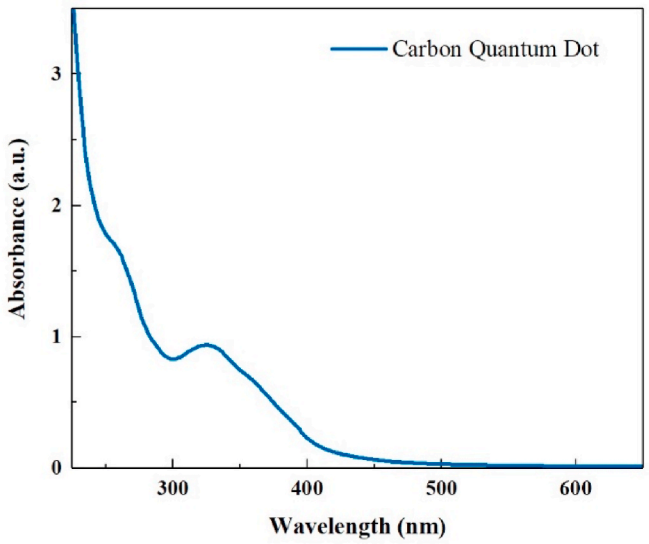


**Fig. 2.** Absorption spectrum of CQDs.

maximum UV absorption peaks at around 250 and 330 nm wavelengths. The strong absorption peak has appeared at 330 nm, and it is much sharper than that of 250 nm which shows homogeneous the particle size due to the sharp peaks. Since amine was used in the synthesis, the amine edge on the surfaces of CQDs was observed. The absorption peaks located at around 330 nm and 250 nm are related to the n-π* transition of C═O and π-π* transition of carbon, respectively [30].

Simultaneously, the aqueous solution of CQDs emitted obvious blue-green fluorescence according to image of the bottle under UV light (365 nm) (Fig. 3a), and the solution appears transparent in daylight. As can be seen from Fig. 3a, the CQDs have very high quantum yield. CQDs were examined under 360 nm excitation wavelength, and the fluorescence emission of CQDs was obtained at around 490 nm under this exciting wavelength. The obtained fluorescence peak of CQDs is strong and almost symmetrical spectrum (Fig. 3b).

The particle size and morphology of CQDs were characterized by a HRTEM. Fig. 4 displays HRTEM images of the CQDs for various magnifications. The CQDs exhibit majority population and spherical shape with average particle size of 5 nm according to HRTEM images. For investigating the size distribution of the CQDs, the obtained CQDs were dissolved in water for measurement with particle sizer. Fig. 4c shows small size distribution and it was understood that particles with a size of around 4–5 nm were formed from Fig. 4a, b, c.

The XRD analysis were performed to perform their structural characterization. Fig. 5 shows wide-angle XRD patterns of CQDs with two broad peaks centered at ~22° and ~42.0°, corresponding to the 002 and 100 lattice planes of a typical amorphous carbon. The broad diffraction peak at ~22° indicates that the interlayer spacing of CQDs is larger than that of graphite, probably it is due to nitrogen-containing groups. To confirm the structure and to perform the surface elemental analysis of the surface of N-doped CQDs, XPS measurements were performed (in Fig. 5b, c, d). The measurement results show that the strong peaks at 533.1 eV, 400.1 eV and 286.5 eV correspond to binding energies of O1s, N 1S and C1s, respectively [31]. In the high resolution spectrum of C1s peaks at 285.7 and 284.5 eV can be assigned to C–N ve C–C bonds, respectively [32].

The N1s peaks located at 398.59, 400.16 and 400.92 eV show that nitrogen exists mostly in the form of C–N═C ($sp^2$), $(C)_3$–N ($sp^3$) and N–H ($sp^3$), respectively and the spectrum confirms that CQDs were successfully functionalized by $–NH_2$ group [33].

### 3.2. Electrochemical analysis of fluorescent CQDs

Electrochemical analysis was started firstly with cyclic voltammetry (CV) measurements. In this section, the possible occurrence of redox reactions in the electrochemical cells was determined in the range of ±1 V by CV. Fig. 6 indicates the CV results for various scan rates for CQDs samples. CV analyzes showed permanent capacitive current plateaus in the range of ± 1 V as electrodes. Also, any Faradaic current or redox reaction peaks were not observed in the CV. The CV profile highlighted that the symmetric capacitors prepared with CQDs electrodes which called Pseudocapacitor feature [34]. In addition, rectangular shape CV patterns as in Fig. 6, which indicate that CQDs symmetric capacitors can be assume like supercapacitors. In CQDs capacitors, when the voltage is applied to the capacitor to charge, $K^+$ (anion) and $OH^-$ (cation), which are ionized in the electrolyte, tend to the electrodes and cause the electrodes to become polarized [35]. This process is reversed in the discharge process, and K+ and OH- ions are transferred to their counter electrode. The intensification of the polarization in the electrodes will directly affect the capacitance due to the electric field that will occur in the capacitor. CV analyzes also show that in polarization formed in CQDs capacitors, $K^+$ or $OH^-$ ions do not make any bonds with the electrodes, they only diffuse to the electrode surface and inner layers and provide polarization.

In the second part of the electrochemical analysis, capacitance calculations were made by long charge-discharge cycles with the help of CV analyses data. Fig. 7a and b shows the capacitance values in the first charge-discharge of CQDs capacitor and cycle life analysis, respectively. According to the first charge-discharge cycle result, CQDs provides 16.2 F/g charge and 8.2 F/g discharge capacitance. These levels capacitance values support the CQDs electrodes showed supercapacitor features [29]. The cycle-life analysis performed at constant voltage sweep rate of 200 mV/s. During the first 10 cycles, there is a significant decrease in charge and discharge capacitance values, and this decrease become stable after the 10th cycle. Table 1 shows the capacitance values of the 1,

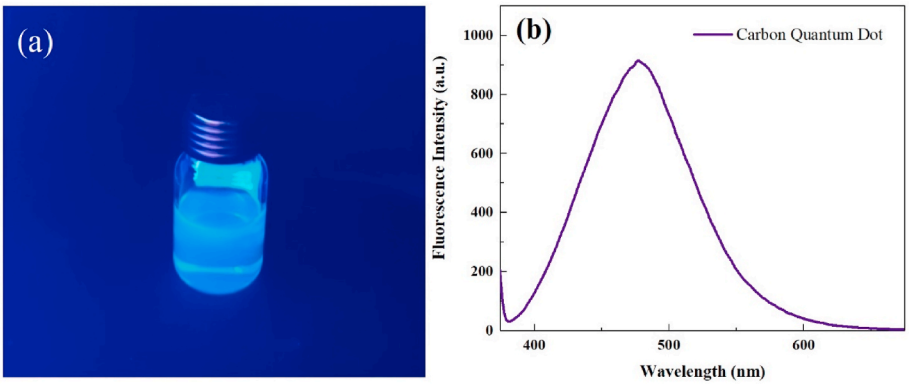


**Fig. 3. a)** Image of CQDs solution under UV light and **b)** fluorescence spectrum of CQDs.

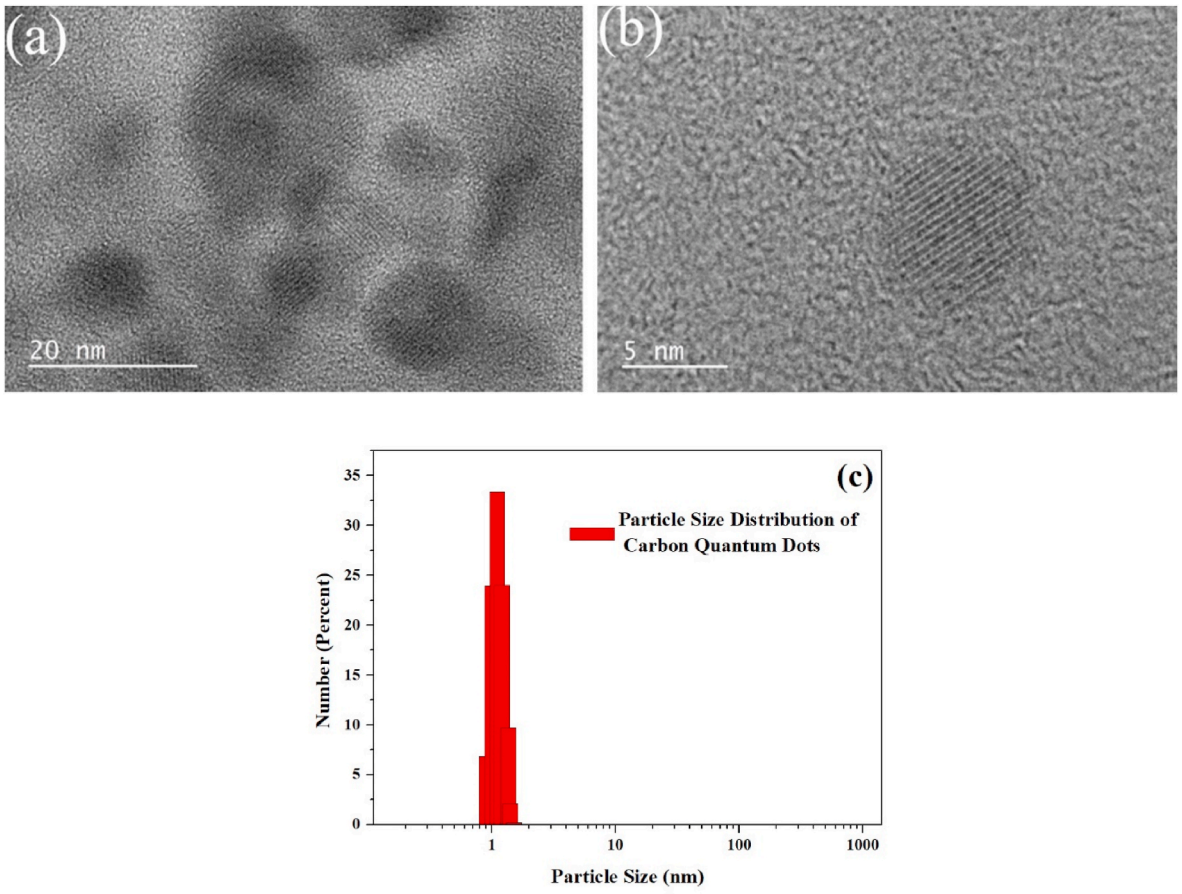


**Fig. 4. a), b)** HRTEM image and **c)** particle size distribution histogram of CQDs.

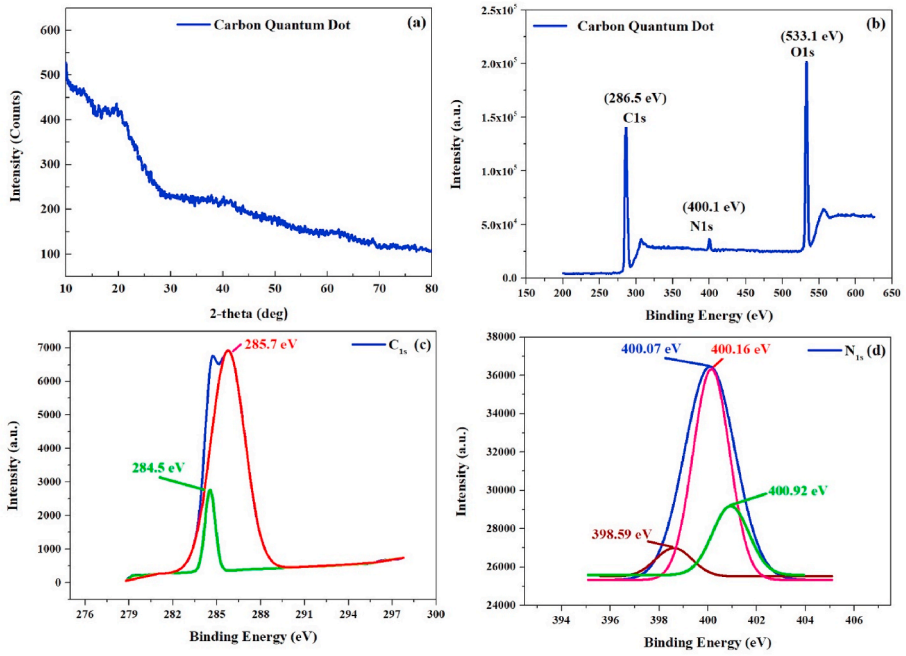


**Fig. 5. a)** XRD pattern and **b)** XPS survey spectrum and XPS deconvolutions **c)** C1s, **d)** N1s for CQDs.

50, 100 and 200th cycles. Especially after the 10th cycle, the capacitance has changed in discharged capacitance values by a very low level. This result reveals that CQDs capacitors show stable capacitive performance at long-term technological usage. Moreover, the capacity retention value has been calculated for CQDs capacitors. The discharge capacitance retention value was calculated as 34.08% at the end of 200

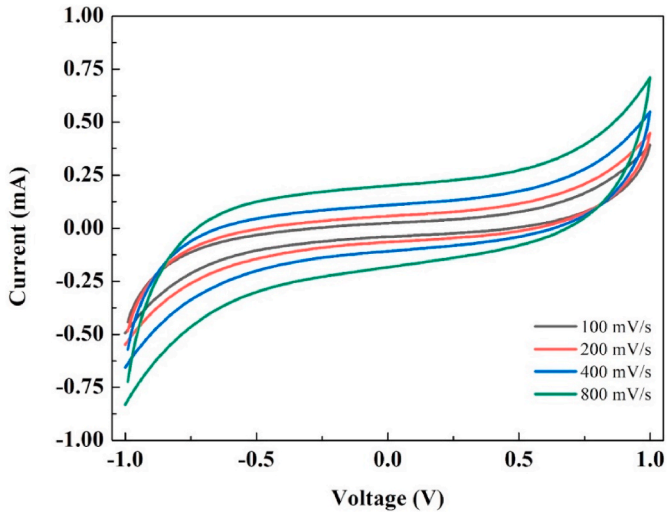


**Fig. 6.** CV analysis at different scan speeds.

cycles and given in Table 1.

Another important point can be seen in the capacitance analysis. There is bigger difference between charge-discharge capacitance values. According to Pseudocapacitor behavior, electrolyte ions pull more charge carrier onto the electrode-electrolyte surface, and that may affect charge-discharge capacitance differences. Similar situation was observed in CQDs capacitors and can be thought the main reason of the capacitance difference between the charge-discharge capacities. Especially much more charge capacitance than discharge capacitance may occur due to the anodic property of the CQDs material [36]. The anodic CQDs electrode can be stored more K+ ions (KOH electrolyte) on the electrode surface (electrode-electrolyte interface) and thus, more electrons can be gathered around K+ ions. Therefore, the material can store much more capacitive charge as charge capacitance [36–38].

According to the literature, the capacitive performance of CQD capacitors is at low levels in some studies, and it is at high levels in other studies. In order to comparison our results with literature the Table- 2 have been prepared. Table- 2 shows the capacitive CQD performance is increased with the production technique, the type of electrolyte and different modifications. Also, the capacitance values, which can vary between 0.24 F/g and 594 F/g, vary according to different current and voltage scanning rates and electrolytes used [39–42]. Especially in the studies indicated in Table- 2 (except for our study), 1 M $H_2SO_4$ acidic electrolyte was used. It has been observed that the electrolyte factor is important in increasing the performance of CQD Capacitors. Table- 2 also shows the comparison of CQD vs CDs/Graphene electrode performances. While CDs/Graphene electrodes provide ~24 F/g capacitance in the 0–3 V range and 100 mV/s scanning rate, in our study, ~15 F/g capacity has been obtained with 200 mV/s scanning speed in the 0–1 V range (Table 2) [42].

Fig. 8 shows the comparison of the capacitance values of CQDs capacitors under various scanning speeds. According to the measurements between 100 and 800 mV/s, higher capacitance values were obtained at lower scanning speeds. Moreover, CQDs capacitors exhibited supercapacitor properties at high speed voltage sweep rates with KOH(aq) electrolyte.

## 4. Conclusion

A new nitrogen-containing carbon quantum dots (CQDs) were derived by a simple and quick synthesis method. CQDs were obtained using fermented tea with Kombucha fungus. The synthesized CQDs showed excellent optical, electrical properties and good stability. To determine optical and structural properties of the CQDs were characterized by UV absorption, fluorescence spectroscopy, HRTEM, particle sizer, XPS and XRD, respectively. The resulting CQDs exhibited intense emission and showed properties to be the favorite material for electronic applications. The CQDs were used as electrode materials for supercapacitor structure and characterized by electrochemical analysis to determine charge-discharge profiles and capacity. The results revealed that the green synthesized CQDs can be employed and improved for supercapacitor applications.

**Table 2**
Comparison of CQD capacitor performances.

| Electrode | Potential Window | Capacitance | Reference |
|---|---|---|---|
| Milk-CQD | 0–0.8 V | 95 F/g (at 0.12 A/g)<br>40 F/g (at 0.2 A/g) | [39] |
| CQD-PPy | (-0.2)-1 V | 0.24 F/g (at 150 mV/s) | [40] |
| RCQD/RuO | 0–1 V | 594 F/g (at 1 A/g) | [41] |
| CDs/Graphene | 0–3 V | 24.15 (at 100 mV/s) | [42] |
| KF-CQDs | 0–1 V | 15.13 F/g (200 mV/s) | This Study |

CQD: Carbon Quantum Dot; CD: Carbon Dot.

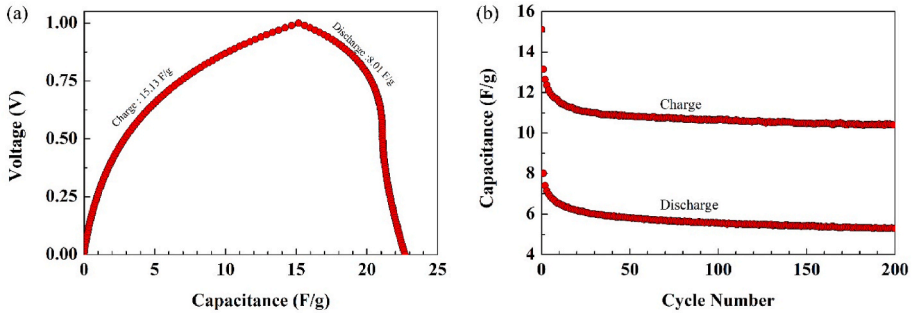


**Fig. 7.** a) 1st cycle charge-discharge characteristic and b) cycle-life analysis.

**Table 1**
Capacitance values and capacity retention value at some specific cycle numbers.

| 1. Cycle | | 50. Cycle | | 100. Cycle | | 200. Cycle | | Ch. Cap. Rtn. % | Dch. Cap. Rtn. % |
|---|---|---|---|---|---|---|---|---|---|
| Ch. | Dch. | Ch. | Dch. | Ch. | Dch. | Ch. | Dch. | | |
| 15.13 | 8.01 | 10.84 | 5.79 | 10.66 | 5.54 | 10.40 | 5.28 | 31.26 | 34.08 |

**Ch** = Charge capacitance (F/g); **Dch** = Discharge capacitance (F/g); **Dch Cap Rtn** = Discharge Capacitance Retention (%).

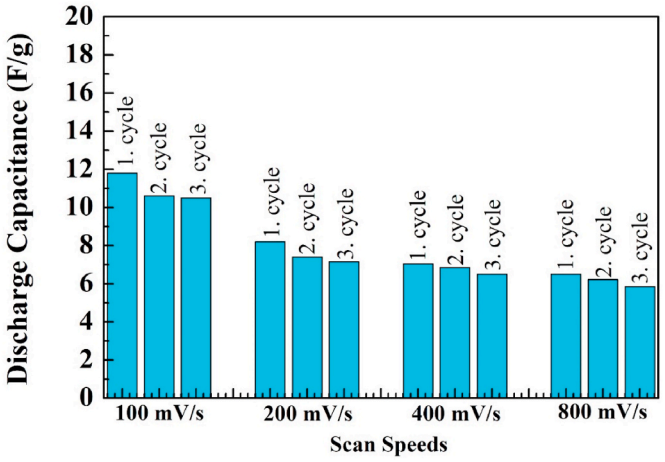


**Fig. 8.** Capacitance analysis under some specific constant voltages.

## CRediT authorship contribution statement

**Canan Başlak:** Writing – review & editing, Writing – original draft, Visualization, Validation, Supervision, Methodology, Investigation, Formal analysis, Data curation, canan Baslak: . **Serkan Demirel:** Writing – review & editing, Writing – original draft, Visualization, Validation, Investigation, Formal analysis. **Adem Kocyigit:** Writing – review & editing, Writing – original draft, Visualization, Validation, Investigation, Formal analysis. **Hamdiye Alatlı:** Investigation, Formal analysis. **Murat Yıldırım:** Writing – review & editing, Writing – original draft, Supervision.

## Declaration of competing interest

The authors declare that they have no known competing financial interests or personal relationships that could have appeared to influence the work reported in this paper.

## References

[1] J. Reiss, Influence of different sugars on the metabolism of the tea fungus, Z. Lebensm. Unters. Forsch. 198 (1994) 258–261, https://doi.org/10.1007/BF01192606.
[2] R. Jayabalan, R.V. Malbaša, E.S. Lončar, J.S. Vitas, M. Sathishkumar, A review on kombucha tea-microbiology, composition, fermentation, beneficial effects, toxicity, and tea fungus, Compr. Rev. Food Sci. Food Saf. 13 (2014) 538–550, https://doi.org/10.1111/1541-4337.12073.
[3] C. Chen, B.Y. Liu, Changes in major components of tea fungus metabolites during prolonged fermentation, J. Appl. Microbiol. 89 (2000) 834–839, https://doi.org/10.1046/j.1365-2672.2000.01188.x.
[4] C. Baslak, Development of fluorescence-based optical sensors for detection of Cr (III) ions in water by using quantum nanocrystals, Res. Chem. Intermed. 45 (2019) 3633–3640, https://doi.org/10.1007/s11164-018-3615-6.
[5] E. Trovatti, L.S. Serafim, C.S.R. Freire, A.J.D. Silvestre, C.P. Neto, Gluconacetobacter sacchari: an efficient bacterial cellulose cell-factory, Carbohydr. Polym. 86 (2011) 1417–1420, https://doi.org/10.1016/j.carbpol.2011.06.046.
[6] G. Jiang, J. Zhang, J. Qiao, Y. Jiang, H. Zarrin, Z. Chen, F. Hong, Bacterial nanocellulose/Nafion composite membranes for low temperature polymer electrolyte fuel cells, J. Power Sources 273 (2015) 697–706, https://doi.org/10.1016/j.jpowsour.2014.09.145.
[7] A.N. May, J. Medina, J. Alcock, C. Maley, A. Aktipis, Kombucha as a model system for multispecies microbial cooperation: theoretical promise, methodological challenges and new solutions 'in solution, bioRxiv (2017) 214478, https://doi.org/10.1101/214478.
[8] D. Kong, F. Yan, Y. Luo, Q. Ye, S. Zhou, L. Chen, Amphiphilic carbon dots for sensitive detection, intracellular imaging of Al3+, Anal. Chim. Acta 953 (2017) 63–70, https://doi.org/10.1016/j.aca.2016.11.049.
[9] S. Pei, J. Zhang, M. Gao, D. Wu, Y. Yang, R. Liu, A facile hydrothermal approach towards photoluminescent carbon dots from amino acids, J. Colloid Interface Sci. 439 (2015) 129–133, https://doi.org/10.1016/j.jcis.2014.10.030.
[10] C.-B. Ma, Z.-T. Zhu, H.-X. Wang, X. Huang, X. Zhang, X. Qi, H.-L. Zhang, Y. Zhu, X. Deng, Y. Peng, Y. Han, H. Zhang, A general solid-state synthesis of chemically-doped fluorescent graphene quantum dots for bioimaging and optoelectronic applications, Nanoscale 7 (2015) 10162–10169, https://doi.org/10.1039/C5NR01757B.
[11] V. Gupta, N. Chaudhary, R. Srivastava, G.D. Sharma, R. Bhardwaj, S. Chand, Luminscent graphene quantum dots for organic photovoltaic devices, J. Am. Chem. Soc. 133 (2011) 9960–9963, https://doi.org/10.1021/ja2036749.
[12] X. Sun, Z. Liu, K. Welsher, J.T. Robinson, A. Goodwin, S. Zaric, H. Dai, Nano-graphene oxide for cellular imaging and drug delivery, Nano Res. 1 (2008) 203–212, https://doi.org/10.1007/s12274-008-8021-8.
[13] Z. Liu, J.T. Robinson, X. Sun, H. Dai, PEGylated nanographene oxide for delivery of water-insoluble cancer drugs, J. Am. Chem. Soc. 130 (2008) 10876–10877, https://doi.org/10.1021/ja803688x.
[14] J.-L. Wang, J.-Y. Teng, T. Jia, Y. Shu, Detection of yeast Saccharomyces cerevisiae with ionic liquid mediated carbon dots, Talanta 178 (2018) 818–824, https://doi.org/10.1016/j.talanta.2017.10.029.
[15] X. Li, S.P. Lau, L. Tang, R. Ji, P. Yang, Multicolour light emission from chlorine-doped graphene quantum dots, J. Mater. Chem. C. 1 (2013) 7308, https://doi.org/10.1039/c3tc31473a.
[16] Z.L. Wu, M.X. Gao, T.T. Wang, X.Y. Wan, L.L. Zheng, C.Z. Huang, A general quantitative pH sensor developed with dicyandiamide N-doped high quantum yield graphene quantum dots, Nanoscale 6 (2014) 3868–3874, https://doi.org/10.1039/C3NR06353D.
[17] Y. Dong, H. Pang, H. Bin Yang, C. Guo, J. Shao, Y. Chi, C.M. Li, T. Yu, Carbon-Based dots Co-doped with nitrogen and sulfur for high quantum yield and excitation-independent emission, Angew. Chem. Int. Ed. 52 (2013) 7800–7804, https://doi.org/10.1002/anie.201301114.
[18] S. Zhu, Q. Meng, L. Wang, J. Zhang, Y. Song, H. Jin, K. Zhang, H. Sun, H. Wang, B. Yang, Highly photoluminescent carbon dots for multicolor patterning, Sensors, and Bioimaging, Angew. Chemie Int. Ed. 52 (2013) 3953–3957, https://doi.org/10.1002/anie.201300519.
[19] T. Purkait, G. Singh, D. Kumar, M. Singh, R.S. Dey, High-performance flexible supercapacitors based on electrochemically tailored three-dimensional reduced graphene oxide networks, Sci. Rep. 8 (2018) 1–13, https://doi.org/10.1038/s41598-017-18593-3.
[20] A. Borenstein, O. Hanna, R. Attias, S. Luski, T. Brousse, D. Aurbach, Carbon-based composite materials for supercapacitor electrodes: a review, J. Mater. Chem. A. 5 (2017) 12653–12672, https://doi.org/10.1039/c7ta00863e.
[21] R. Fields, C. Lei, F. Markoulidis, C. Lekakou, The composite supercapacitor, Energy Technol. 4 (2016) 517–525, https://doi.org/10.1002/ente.201500328.
[22] N. Choudhary, C. Li, J. Moore, N. Nagaiah, L. Zhai, Y. Jung, J. Thomas, Asymmetric supercapacitor electrodes and devices, Adv. Mater. 29 (2017) 1605336, https://doi.org/10.1002/adma.201605336.
[23] K. Kakaei, S. Khodadoost, M. Gholipour, N. Shouraei, Core-shell polyaniline functionalized carbon quantum dots for supercapacitor, J. Phys. Chem. Solid. 148 (2021) 109753, https://doi.org/10.1016/j.jpcs.2020.109753.
[24] J. Xiao, R. Momen, C. Liu, Application of carbon quantum dots in supercapacitors: a mini review, Electrochem. Commun. 132 (2021) 107143, https://doi.org/10.1016/j.elecom.2021.107143.
[25] Y. Yang, Y. Wang, L. Zhao, Y. Liu, F. Ran, Visualizing nucleation and growth process of vanadium-supramolecular nanoribbons self-assembled by rapid cooling method towards high-capacity vanadium nitride anode materials, Adv. Energy Mater. 12 (2022) 2103158, https://doi.org/10.1002/aenm.202103158.
[26] Y. Liu, L. Liu, L. Kang, F. Ran, Energy storage mechanism of vanadium nitride via intercalating different atomic radius for expanding interplanar spacing, ENERGY Environ. Mater. (2021) 12188, https://doi.org/10.1002/eem2.12188, eem2.
[27] Ç. Kırbıyık, A. Toprak, C. Başlak, M. Kuş, M. Ersöz, Nitrogen-doped CQDs to enhance the power conversion efficiency of perovskite solar cells via surface passivation, J. Alloys Compd. 832 (2020) 154897, https://doi.org/10.1016/j.jallcom.2020.154897.
[28] C. Baslak, A.N. Kursunlu, New optical sensor based on pillar[5]Arene-carbon quantum dot composite material, in: III. Int. Sci. Vocat. Stud. Congr. – Sci. Heal., BILMES SH, 2019, pp. 34–37, 2019.
[29] K. Cicek, S. Demirel, Self-healable PVA–graphite–borax as electrode and electrolyte properties for smart and flexible supercapacitor applications, J. Mater. Sci. Mater. Electron. 32 (2021) 16335–16345, https://doi.org/10.1007/s10854-021-06186-w.
[30] P. Lv, Y. Yao, H. Zhou, J. Zhang, Z. Pang, K. Ao, Y. Cai, Q. Wei, Synthesis of novel nitrogen-doped carbon dots for highly selective detection of iron ion, Nanotechnology 28 (2017) 165502, https://doi.org/10.1088/1361-6528/aa6320.
[31] Y. Qiang, S. Zhang, H. Zhao, B. Tan, L. Wang, Enhanced anticorrosion performance of copper by novel N-doped carbon dots, Corrosion Sci. 161 (2019) 108193, https://doi.org/10.1016/j.corsci.2019.108193.
[32] Y.-F. Kang, Y.-H. Li, Y.-W. Fang, Y. Xu, X.-M. Wei, X.-B. Yin, Carbon quantum dots for zebrafish fluorescence imaging, Sci. Rep. 5 (2015) 11835, https://doi.org/10.1038/srep11835.
[33] Y.R. Park, H.Y. Jeong, Y.S. Seo, W.K. Choi, Y.J. Hong, Quantum-Dot light-emitting diodes with nitrogen-doped carbon nanodot hole transport and electronic energy transfer layer, Sci. Rep. 7 (2017) 46422, https://doi.org/10.1038/srep46422.
[34] Y. Jiang, J. Liu, Definitions of pseudocapacitive materials: a brief review, Energy Environ. Mater. 2 (2019) 30–37, https://doi.org/10.1002/eem2.12028.
[35] P. Simon, Y. Gogotsi, Charge storage mechanism in nanoporous carbons and its consequence for electrical double layer capacitors, Philos. Trans. R. Soc. A Math. Phys. Eng. Sci. 368 (2010) 3457–3467, https://doi.org/10.1098/rsta.2010.0109.
[36] D. Chen, S.R. Bishop, H.L. Tuller, Nonstoichiometry in oxide thin films operating under anodic conditions: a chemical capacitance study of the praseodymium-cerium oxide system, Chem. Mater. 26 (2014) 6622–6627, https://doi.org/10.1021/cm503440v.

[37] C.W. Sun, S.S. Hsiau, Effect of electrolyte concentration difference on hydrogen production during pem electrolysis, J. Electrochem. Sci. Technol. 9 (2018) 99–108, https://doi.org/10.5229/JECST.2018.9.2.99.

[38] V.A. Nikitina, S.M. Kuzovchikov, S.S. Fedotov, N.R. Khasanova, A.M. Abakumov, E. V. Antipov, Effect of the electrode/electrolyte interface structure on the potassium-ion diffusional and charge transfer rates: towards a high voltage potassium-ion battery, Electrochim. Acta 258 (2017) 814–824, https://doi.org/10.1016/j.electacta.2017.11.131.

[39] M. Athika, A. Prasath, E. Duraisamy, V. Sankar Devi, A. Selva Sharma, P. Elumalai, Carbon-quantum dots derived from denatured milk for efficient chromium-ion sensing and supercapacitor applications, Mater. Lett. 241 (2019) 156–159, https://doi.org/10.1016/j.matlet.2019.01.064.

[40] S. Sagar Mittal, G. Ramadas, N. Vasanthmurali, V.S. Madaneshwar, M. Sathish Kumar, N.K. Kothurkar, Carbon quantum dot-polypyrrole nanocomposite for supercapacitor electrodes, IOP Conf. Ser. Mater. Sci. Eng. 577 (2019), 012194, https://doi.org/10.1088/1757-899X/577/1/012194.

[41] Y. Zhu, X. Ji, C. Pan, Q. Sun, W. Song, L. Fang, Q. Chen, C.E. Banks, A carbon quantum dot decorated RuO2 network: outstanding supercapacitances under ultrafast charge and discharge, Energy Environ. Sci. 6 (2013) 3665, https://doi.org/10.1039/c3ee41776j.

[42] Q. Li, H. Cheng, X. Wu, C.-F. Wang, G. Wu, S. Chen, Enriched carbon dots/graphene microfibers towards high-performance micro-supercapacitors, J. Mater. Chem. A. 6 (2018) 14112–14119, https://doi.org/10.1039/C8TA02124D.